

# Local correlation functions of arbitrary order for the Falicov-Kimball model

T. Ribic<sup>1</sup>, G. Rohringer<sup>1,2</sup>, and K. Held<sup>1</sup>

<sup>1</sup>*Institute of Solid State Physics, TU Wien, 1040 Vienna, Austria ,*

<sup>2</sup>*Russian Quantum Center, Novaya street, 100, Skolkovo, Moscow region 143025, Russia*

(Dated: Version 0.95, December 12, 2016)

Local  $n$ -particle vertex function represent the crucial ingredient for all diagrammatic extensions of dynamical mean field theory (DMFT). Hitherto their application has been restricted -with a few exceptions- to the  $n = 2$ -particle vertex while higher-order vertices have been neglected. In this paper we derive a general analytical expression for the  $n$ -particle (one-particle reducible) vertex of the Falicov-Kimball model (FKM). We observe that the magnitude of such vertex functions itself strongly increases with the particle-number  $n$ . On the other hand, their effect on generic Feynman diagrams remains rather moderate due to the damping effect of the Green's functions present in such diagrams. Nevertheless, they yield important contributions to the self-energy corrections calculated in diagrammatic extensions of DMFT as we explicitly demonstrate using the example of dual fermion (DF) calculations for the two-dimensional FKM at quarter filling of stationary  $f$ -electrons where corrections to the self-energy obtained from the three-particle vertex are indeed comparable in magnitude to corresponding corrections stemming from the two-particle vertex.

PACS numbers: 71.27.+a, 71.10.Fd

## I. INTRODUCTION

With the establishment of dynamical mean field theory (DMFT)<sup>1–5</sup> as a state-of-the-art method for calculating strongly correlated electron models<sup>5</sup> and materials<sup>6,7</sup>, the scientific frontier moved on to extensions of DMFT that include the important local correlations of DMFT but also non-local correlations beyond. One route to this end are cluster extensions of DMFT where a finite cluster of sites is surrounded by a DMFT bath<sup>8–11</sup>. More recently, diagrammatic extensions of DMFT have been proposed as a vivid alternative<sup>12–15,17</sup>, which have in particular the advantage that long-range and short-range correlations are treated on an equal footing and that realistic materials calculations<sup>18</sup> are possible. Note that the numerical effort of cluster extensions generally grows exponentially with the number of sites times the number of orbitals, which severely restricts the application of cluster extensions.

Several closely related diagrammatic extensions of DMFT have been proposed: the dynamical vertex approximation (DFA)<sup>12–14</sup>, the dual fermion (DF)<sup>15</sup>, dual boson<sup>16</sup> and non-local expansion<sup>19</sup>, the one-particle irreducible approach (1PI)<sup>20</sup>, the merger of DMFT with the functional renormalization group (DMF<sup>2</sup>RG)<sup>21</sup>, the triply- and quadruply-irreducible local expansion<sup>22,23</sup> and DMFT+fluctuation exchange (FLEX)<sup>24</sup>. All these approaches start from the local, but fully frequency dependent vertex, and diagrammatically construct from this non-local correlations beyond DMFT. Particular highlights of the results obtained using these novel approaches are so-far: the calculation of the critical<sup>27,28</sup> and quantum critical<sup>29</sup> exponents of the Hubbard model and those of the Falicov Kimball model<sup>30</sup>, as well as establishing the insulating nature of the paramagnetic phase in the half-filled Hubbard model on a square lattice at arbitrarily small interactions<sup>31</sup>.

The DF and 1PI approach constitute a systematic expansion of the self-energy of the system in local one-, two- and more-particle local correlation (vertex) functions which is, in principle, exact when including *all*  $n$ -particle vertices in the calculation. But in practice, these approaches are truncated at the two-particle vertex level which constitutes the most fundamental approximation regarding these vertex approaches<sup>32</sup>. The main reason for this truncation is that the complexity and numerical effort is already at the edge of what is possible for the  $n = 2$  particle vertex, for which the full dependence on three frequencies needs to be taken into account<sup>41</sup>. At least this is true for the Hubbard model within DMFT, where arguably the most efficient way to calculate the corresponding local two-particle vertex is by means of quantum Monte-Carlo simulations<sup>42–44</sup> with worm sampling<sup>45</sup> and improved estimators<sup>46</sup>. While individual contributions of the local three-particle vertex of the DMFT Hubbard or impurity model have been calculated this way<sup>46</sup>, obtaining its full dependence on five frequencies exceeds presently available resources regarding both, computational time and memory.

The Falicov Kimball model (FKM)<sup>47</sup> on the other hand has a much simpler structure than the Hubbard model. In contrast to the latter it describes noninteracting itinerant electrons which are scattered at localized ones and, hence, represent a model for (annealed) disorder rather than “real” correlations. Due to this reduced structure it has a long tradition of (semi-)analytical calculations that are not possible for the Hubbard model. Therefore, the FKM has been commonly utilized as a test-bed for new approaches and concepts. Indeed the FKM can be solved analytically in DMFT<sup>48,49</sup>, including charge density wave ordering<sup>50</sup> and transport properties<sup>51</sup>. Vertex corrections to the conductivity<sup>52,53</sup> and Anderson localization<sup>54</sup> have been discussed ; and it has been studied in DF<sup>30</sup> and 1PI<sup>55</sup>. The analytical calculation of the local two-

particle vertex of the FKM<sup>49,55,56</sup> shows a much simpler, reduced frequency structure in comparison to the Hubbard model<sup>41</sup>. That is, the two-particle vertex has only two contributions since no energy can be transferred to the localized electrons: (i) an  $\omega \neq 0$  ( $\omega$ : transferred bosonic frequency) contribution where the two fermionic frequencies have to be the same  $\nu = \nu'$ <sup>49</sup> and (ii) an  $\omega = 0$  contribution<sup>55,56</sup>.

In this paper, we analytically calculate the full  $n$ -particle vertex of the FKM for arbitrary  $n$  and analyze its magnitude as a function of  $n$ . This is a very relevant issue since the typical truncation of the self-energy in the DF and 1PI theory at the two-particle vertex level relies on the “smallness” of higher-order vertex functions. We, hence, finally investigate the importance of such higher-order vertices exemplary in the DF theory by including the  $n = 3$  particle vertex in the DF correction to the DMFT self-energy. While at half-filling this three-particle vertex vanishes it yields a sizable contribution to the nonlocal DF correction of the DMFT self-energy in the case of quarter filling, indicating that in a general situation some caution has to be taken when cutting the DF expansion at the two-particle vertex level.

The outline of our paper is the following: In Section II, we derive the analytical formula for the  $n$ -particle connected Green’s and vertex functions of the FKM within DMFT. To this end, we first calculate in Section II A the  $n$ -particle Green’s function, from which we remove all disconnected contributions (Secs. II B and II C). In Section III we analyze how the prefactor of the  $n$ -particle vertex grows with  $n$  and provide an analytic estimate for its asymptotic behavior. From this we deduce in Sec. IV the magnitude of the contribution of such vertices in generic self-energy diagrams of DF and 1PI. In Section V we then calculate some selected correction terms for the DF self-energy stemming from the  $n = 3$  particle vertex and compare them to the corresponding more standard corrections from two-particle vertex functions only. Finally, Section VI is devoted to a summary of our main results and an outlook.

## II. ANALYTIC DERIVATION OF THE $n$ -PARTICLE VERTEX IN THE FKM

The Hamiltonian of the spin-less (one-band) Falicov Kimball model reads

$$\hat{\mathcal{H}} = -t \sum_{\langle ij \rangle} \hat{c}_i^\dagger \hat{c}_j + U \sum_i \hat{c}_i^\dagger \hat{c}_i \hat{f}_i^\dagger \hat{f}_i + \mu_c \sum_i \hat{c}_i^\dagger \hat{c}_i + \mu_f \sum_i \hat{f}_i^\dagger \hat{f}_i \quad (1)$$

where  $\hat{c}_i^{(\dagger)}$  annihilates (creates) an itinerant  $c$ -electron and, correspondingly,  $\hat{f}_i^{(\dagger)}$  annihilates (creates) a localized  $f$ -electron at the lattice site  $i$ ;  $t$  represents the hopping amplitude for a mobile electron between nearest-neighbor sites  $\langle ij \rangle$ . The two electron species interact with each other via a purely local (Hubbard-like) interaction parametrized by the interaction strength  $U$ ;  $\mu_c$  and  $\mu_f$

denote the chemical potentials for the itinerant and localized electrons, respectively, which determine the density of the corresponding particles. Throughout the paper all energies will be measured in terms of  $4t$  representing the half band-width for the FKM on a  $2d$  square lattice;  $T = 1/\beta$  is the temperature.

In the following we will consider the DMFT solution of model (1) and derive analytical expressions for the corresponding local (connected)  $n$ -particle DMFT vertex function for arbitrary  $n$ . To this end we systematically subtract all disconnected contributions from the full  $n$ -particle Green’s function  $G^{(n)}$ . As we will show, this is achieved by a two-step procedure where (i) all diagrams which can be written as a product of a one-particle Green’s function  $G^{(1)}$  and a remainder are eliminated from  $G^{(n)}$ . Then we (ii) remove in the second step all disconnected products among purely higher-particle Green’s functions ( $G^{(2)}, G^{(3)}, \dots$ ) which yields -after amputating the outer legs via dividing by the corresponding one-particle Green’s functions  $G^{(1)}$ - the final result for the  $n$ -particle local DMFT vertex function for the FKM.

Let us stress that all results and derivations presented in this section are independent of the underlying lattice type (e.g., square, cubic, Bethe, etc.). The density of itinerant and localized electrons only enters through the local one-particle Green’s function.

### A. Calculation of DMFT $n$ -particle Green’s functions

Let us start our considerations by recalling that the (local) single particle Green’s function of the FKM in the framework of DMFT is just given as

$$G(a) = p_1 \underbrace{\frac{1}{ia + \mu_c - \Delta(a) - U}}_{\equiv \tilde{G}(a)} + p_2 \underbrace{\frac{1}{ia + \mu_c - \Delta(a)}}_{\equiv \tilde{G}(a)}, \quad (2)$$

where  $a = \pi T(2n_a + 1)$ ,  $n_a \in \mathbb{Z}$ , is a fermionic Matsubara frequency and  $\Delta(a)$  denotes the hybridization function of DMFT.  $\tilde{G}(a)$  represents the (non-interacting) single-particle Green’s function for the itinerant  $c$  electrons if no localized  $f$ -electron is present at the impurity site;  $\tilde{G}(a)$  corresponds to the same (non-interacting) Green’s function but in the presence of a localized electron which, however, just increases the energy level for the itinerant one by  $U$ . Here, the weight  $p_1 = \langle \hat{f}^\dagger \hat{f} \rangle$  corresponds to the density of localized electrons at each lattice site (i.e., to the probability for finding such an electron at the given site) and  $p_2 = 1 - p_1$ . Hence, the local DMFT single-particle Green’s function for the itinerant electrons is given just by the weighted average of non-interacting Green’s functions in the presence (absence) of a localized electron which, hence, acts merely as a scattering potential for the itinerant particles.

This non-interacting-like nature of the FKM allows

for a straightforward determination of the  $n$ -particle Green's functions. In fact, taking into account that in the non-interacting situation the latter is -due to Wicks theorem- just a sum of all possible products of single-particle Green's functions (i.e., considering all possible frequency permutations of in- and outgoing particles), we can express the general  $n$ -particle correlation function for the FKM -analogously as in the one-particle case- by a weighted average over the corresponding non-interacting quantities in the presence ( $\tilde{G}$ ) and absence ( $G$ ) of a localized electron. This leads to the following expression for the local DMFT  $n$ -particle Green's function of the FKM<sup>25</sup>

$$G^{(n)}(a_1, a_2, \dots, a_n; a_{n+1}, a_{n+2}, \dots, a_{2n}) = \delta_{a_{n+1} \dots a_{2n}}^{a_1 \dots a_n} \left[ p_1 \left( \tilde{G}(a_1) \tilde{G}(a_2) \dots \tilde{G}(a_n) \right) + p_2 \left( G(a_1) G(a_2) \dots G(a_n) \right) \right], \quad (3)$$

where  $a_1, a_2 \dots a_n$  correspond to the  $(n)$  frequencies of the incoming and  $a_{n+1}, a_{n+2} \dots a_{2n}$  to the  $(n)$  frequencies of the outgoing particles.  $\delta_{a_{n+1} \dots a_{2n}}^{a_1 \dots a_n}$  denotes a generalized Kronecker delta which guarantees energy (frequency) conservation: It is 1 if the entering frequencies are an even permutation of the leaving ones, -1 if they are an odd permutation and 0 otherwise. Moreover, it will be 0 if an incoming/outgoing frequency appears more than once.

Eq. (3) corresponds to the *full* local DMFT  $n$ -particle Green's function and, hence, contains contributions from disconnected as well as from fully connected diagrams. To extract the latter -and from this the  $n$ -particle vertex- we have to remove all disconnected contributions from Eq. (3). At first glance, the most direct way to achieve this seems to be simply to subtract all terms of the form  $G^{(m_1)} \dots G^{(m_k)}$  with  $\sum_{l=1}^k m_l = n$  for all possible partitions  $m_l$  and all possible frequency assignments for a given partition. Such a procedure, however, would lead to a massive over-counting of subtraction terms as one can easily see from the following argument: Consider for instance the contributions  $G^{(1)} G^{(n-1)}$  and  $G^{(2)} G^{(n-2)}$  which certainly have to be subtracted from  $G^{(n)}$ . However, considering that in the first term  $G^{(n-1)}$  includes a contribution  $G^{(1)} G^{(n-2)}$  and in the second term  $G^{(2)}$  contains  $G^{(1)} G^{(1)}$  it becomes obvious that the expression  $G^{(1)} G^{(1)} G^{(n-2)}$  appears in *both* subtraction terms which indeed leads to the above mentioned over-counting problem when naively removing such contributions.

In the following, we will, hence, take another path trying to avoid the above mentioned "over-subtraction". To this end, let us first consider the following algebraic

identities for  $G(a)$ ,  $\tilde{G}(a)$  and  $\tilde{G}(a)$ :

$$\begin{aligned} \tilde{G}(a) &= p_1 \tilde{G}(a) + p_2 \tilde{G}(a) + p_2 G(a) - p_2 G(a) \\ &= G^{(1)}(a) + p_2 [\tilde{G}(a) - G(a)] \end{aligned} \quad (4)$$

$$\begin{aligned} G(a) &= p_1 G(a) + p_2 G(a) + p_1 \tilde{G}(a) - p_1 \tilde{G}(a) \\ &= G^{(1)}(a) - p_1 [\tilde{G}(a) - G(a)]. \end{aligned} \quad (5)$$

Substituting these relations into Eq. (3) recasts the expression of the  $n$ -particle Green's function and yields 2 (from the original two terms) times  $2^n$  (number of possible combinations of terms from the binomials) terms of the structure

$$(\tilde{G} - G)^{l''} G^{(1)^{n-l''}}, \quad (6)$$

which have to be summed up. Note that the expression for a summand as given in Eq. 6 represents a pure symbolic notation with the exponents " $l''$ " and " $n-l''$ " denoting the number of factors of a given type appearing in a single term, without explicitly specifying which frequencies ( $a, b, c, \dots$ ) they are associated with. Obviously, each such term appears exactly twice in the sum [(corresponding to the original two summands in Eq. (3)], once with  $p_1(p_2)^l$  and once with  $p_2(-p_1)^l$  as a prefactor. Hence, we define the factor  $\mathcal{F}_l$ .

$$\mathcal{F}_l = p_1(p_2)^l + p_2(-p_1)^l, \quad (7)$$

which is associated with each summand consisting of a product of  $l$  terms of type  $(\tilde{G} - G)$  and  $n - l$  terms of type  $G^{(1)}$ . This definition allows us to express  $G^{(n)}$  in the following way:

$$G^{(n)} = \delta_{a_{n+1} \dots a_{2n}}^{a_1 \dots a_n} \sum_{l=0}^n \sum_P \mathcal{F}_l (\tilde{G} - G)(a_{P(1)}) \dots (\tilde{G} - G)(a_{P(l)}) \cdot G^{(1)}(a_{P(l+1)}) G^{(1)} \dots G^{(1)}(a_{P(n)}) \frac{1}{l!(n-l)!}, \quad (8)$$

where  $P$  denotes all permutations of the numbers  $i = 1 \dots n$ . The factors  $(n)!$  and  $(n-l)!$  compensate for over-counting due to permutations which only exchange frequencies between the same type ( $G^{(1)}$  or  $(\tilde{G} - G)$ ) of term. For the sake of a better readability of the following derivations we introduce the following (symbolic) shorthand notation for the terms in the sum of Eq. (8):

$$G^{(n)} = \sum_{l=0}^n \binom{n}{l} \mathcal{F}_l (\tilde{G} - G)^{l''} G^{(1)^{n-l''}}, \quad (9)$$

where the combinatorial factor  $\binom{n}{l}$  indicates the summation over all  $\binom{n}{l}$  permutations of the frequencies  $a_1 \dots a_n$

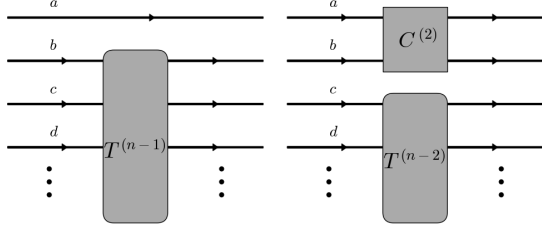


FIG. 1. (Color online) All diagrams where only the frequency  $a$  is 1PD (left) and all the diagrams contributing to the  $n$ -particle one-particle-connected propagator  $T^{(n)}$  where frequency  $a$  is connected only to the frequency  $b$ . (right)

in Eq. (8).

### B. First part of the diagrammatic decomposition

Eq. (9) represent an -up to this point algebraic- decomposition of the full two-particle Green's function. Let us now analyze to which extent the latter already corresponds to a diagrammatic separation of terms. We first introduce the concept of one-particle disconnectedness: Diagrams in which a single Green's function line (with frequency  $a$ ) is disconnected from the rest will be called one-particle disconnected (1PD) (in frequency  $a$ )<sup>78</sup>. The form of Eq. (9) suggests that it already represents a decomposition of  $G^{(n)}$  into 1PD diagrams and a remainder. In fact, the summands for  $l = 0 \dots n-1$  contain a product of one-particle Green's function  $G^{n-l}$  and a -not yet interpreted- contribution  $(\tilde{G} - G)^{l'}$ . Hence, we assume that the terms for  $l = 1 \dots n-1$  contain *all* 1PD diagrams while the remainder  $l = n$  is one-particle connected (i.e., it exhibits no 1PD contributions). The latter will be denoted in the following as

$$T^{(n)}(a_1, \dots, a_n, a_{n+1}, \dots, a_{2n}) = \mathcal{F}_n \delta_{a_{n+1} \dots a_{2n}}^{a_1 \dots a_n} (\tilde{G}(a_1) - G(a_1)) \dots (\tilde{G}(a_n) - G(a_n)), \quad (10)$$

and is illustrated diagrammatically in the left panel of Fig. 1(left) for the diagrammatic representation. We will now prove the above assumption, i.e., that  $T^{(n)}$  indeed corresponds to the sum of all one-particle connected diagrams in  $G^{(n)}$ , by induction. Let us start from the base case  $n = 2$  for which in Ref. 55 we have calculated the full vertex. Since for  $n = 2$  all disconnected diagrams are 1PD,  $T^{(2)}$  is the same as the vertex with external legs

(Green's function lines) and reads [Eq. (6) of 55]:

$$\begin{aligned} T^{(2)}(a_1, a_2; a_3, a_4) &= \delta_{a_3 a_4}^{a_1 a_2} \mathcal{F}_2 (\tilde{G}(a_1) - G(a_1)) (\tilde{G}(a_2) - G(a_2)) \\ &= \delta_{a_3 a_4}^{a_1 a_2} p_1 p_2 (\tilde{G}(a_1) - G(a_1)) (\tilde{G}(a_2) - G(a_2)) \\ &= G^{(1)} G^{(1)} F G^{(1)} G^{(1)} \end{aligned} \quad (11)$$

with  $F$  defined via the equation

$$G^{(2)}(a_1, a_2; a_3, a_4) = \delta_{a_3 a_4}^{a_1 a_2} G^{(1)}(a_1) G^{(1)}(a_2) + G^{(1)} G^{(1)} F G^{(1)} G^{(1)}. \quad (12)$$

The frequency arguments of the expression  $G^{(1)} G^{(1)} F G^{(1)} G^{(1)}$  have been omitted for brevity in both cases. Obviously, Eq. (11) demonstrates that our induction hypothesis, i.e., that  $T^{(n)}$  corresponds to a sum of all one-particle connected diagrams, is correct for  $n = 2$ . Moreover, from Eqs. (9) and (10) we have that

$$T^{(n+1)} = G^{(n+1)} - \sum_{l=0}^n \binom{n}{l} T^{(l)} G^{(1) "n-l+1"}. \quad (13)$$

Since, by the induction hypothesis,  $T^{(l)}$  contains *all* one-particle connected diagrams the term which is subtracted on the r.h.s. of Eq. (13) indeed is identical to the sum of *all* 1PD diagrams in  $G^{(n+1)}$ . Consequently our induction step shows that  $T^{(n+1)}$  does *not* contain any 1PD diagram. Instead it includes all one-particle connected diagrams of  $G^{(n+1)}$  which completes our inductive proof.

Before we proceed with our decomposition procedure by removing the remaining disconnected contributions of  $G^{(n)}$ , let us point out some properties of the one-particle-connected  $n$ -particle propagator.

- For  $n = 2$  and  $n = 3$ ,  $T^{(n)}$  already represents the fully connected contribution to  $G^{(n)}$  as in these cases all disconnected diagrams are 1PD.
- For odd  $l$  and half-filling ( $p_1 = p_2 = 1/2$ ),  $\mathcal{F}_l = 0$  and hence  $T^{(l)} = 0$ . This also implies that the fully connected propagator and by extension the vertex have to vanish as will be discussed in the next section.

### C. Second part of the diagrammatic decomposition

While the term  $T^{(n)}$  derived in the previous section [see Eq. (10)] contains no 1PD diagrams, this does not automatically mean that it already corresponds to the fully connected part of the  $n$ -particle Green's function (as it is indeed the case for  $n = 2$  and  $n = 3$ ). For instance,  $G^{(4)}$  contains -apart from 1PD parts- a disconnected (but not 1PD) contribution proportional to  $T^{(2)} T^{(2)}$  which is a product of one-particle connected diagrams and, hence, still included in  $T^{(4)}$ . Hence, in order to obtain the fully

connected part of  $G^{(n)}$ , which we will denote as  $C^{(n)}$  in the following, we have to remove such contributions. We will do this in the following in two steps: (i) We will derive the general functional form for  $C^{(n)}$  leaving the appropriate prefactor still undefined. (ii) The prefactor will be then determined in the second step by an explicit subtraction of all disconnected diagrams from  $T^{(n)}$ .

(i) As for the first step we realize that for  $n = 2$  and  $n = 3$  the fully connected part of  $G^{(n)}$  is proportional to  $T^{(2)}$  and  $T^{(3)}$ , respectively, i.e., to  $(\tilde{G} - G)^{n-2}$  and  $(\tilde{G} - G)^{n-3}$ , as we have discussed above. This suggests the ansatz

$$\begin{aligned} C^{(n)}(a_1, \dots, a_n, a_{n+1}, \dots, a_{2n}) &= \\ &= \mathcal{C}_n \left( \tilde{G}(a_1) - G(a_1) \right) \dots \left( \tilde{G}(a_n) - G(a_n) \right), \end{aligned} \quad (14)$$

where we have again suppressed the generalized Kronecker symbol  $\delta_{a_{n+1} \dots a_{2n}}^{a_1 \dots a_n}$ ;  $\mathcal{C}_n$  is a -for the moment- unknown constant. We can now prove the assumption made in Eq. (14) for the functional form of the fully connected  $n$ -particle Green's function by induction.

The correctness of Eq. (14) for the base clause, i.e., for  $n = 2$ , follows from Eq. (11). For the induction step, we consider Eq. (14) as induction hypothesis for all  $l = 1 \dots n$  and infer from this, in the following, its correctness for  $n + 1$ . The fully connected  $n + 1$  particle Green's function  $C^{(n+1)}$  can be obtained from the corresponding one-particle connected one  $T^{(n+1)}$  by removing all disconnected diagrams still present in this expression. The latter can be written (due to the absence of 1PD contributions) as products of fully connected  $1, 2, \dots, n$  particle Green's function, i.e.,  $C^{(m_1)} \dots C^{(m_k)}$  where  $2 < m_i \leq n - 2$  and  $\sum_{i=1}^k m_i = n + 1$ . To obtain all terms that need to be subtracted one has to sum over all possible Feynman diagrams of this type, i.e., over all partitions  $m_i$  of  $n + 1$  and -for each such partition- over all possible frequency assignments to the single terms  $C^{(m_i)}$  in the product. The crucial point is now that, since by the induction hypothesis each of the  $C^{(m_i)} \sim (\tilde{G} - G)^{m_i}$ , all the corresponding products in the sum are proportional to  $(\tilde{G}(a_1) - G(a_1)) \dots (\tilde{G}(a_{n+1}) - G(a_{n+1}))$ , where each of the incoming frequencies  $a_1, \dots, a_{n+1}$  is assigned to exactly one of the factors  $(\tilde{G} - G)$ . The only difference lies in the different prefactors of  $(\tilde{G}(a_1) - G(a_1)) \dots (\tilde{G}(a_{n+1}) - G(a_{n+1}))$  for different terms in the sum. Moreover, since also  $T^{(n+1)}$  (from which all these unconnected terms have to be subtracted) has the same structure [see Eq. (10)], the same must hold for  $C^{(n+1)}$  which concludes our proof.

(ii) After we have identified the functional form of  $C^{(n)}$  as given in Eq. (14) we are left with the second (and final) task of determining the prefactor  $\mathcal{C}_n$ . To this end

we will present a diagrammatic procedure that removes systematically from the one-particle connected part of  $G^{(n)}$ , i.e.,  $T^{(n)}$ , all disconnected contributions. This will be achieved by choosing (without loss of generality) one "reference"-frequency, say  $a_1$ , and classify all subtracted (disconnected) diagrams with respect to this frequency.

Let us start with disconnected diagrams where the frequency  $a_1$  is connected only to one other frequency  $a_2$  and the remaining frequencies  $a_3, a_4, \dots$  belong to all possible (one-particle disconnected)  $(n - 2)$ -particle diagrams. As was shown in Sec. II B the latter corresponds exactly to  $T^{(n-2)}(a_3, a_4, \dots)$ . The corresponding subtraction term is depicted in the right panel of Fig. 1 and reads algebraically

$$\begin{aligned} C^{(2)}(a_1, a_2) T^{(n-2)}(a_3, a_4, \dots) &= \mathcal{C}_2 \mathcal{F}_{(n-2)} \left( \tilde{G}(a_1) - G(a_1) \right) \\ &\times \left( \tilde{G}(a_2) - G(a_2) \right) \left( \tilde{G}(a_3) - G(a_3) \right) \left( \tilde{G}(a_4) - G(a_4) \right) \dots, \end{aligned} \quad (15)$$

where  $\dots$  denotes the multiplication with terms of the type  $(\tilde{G} - G)$  for all remaining frequencies. In the same way a disconnected contribution, where the frequency  $a_1$  is connected only to frequency  $a_3$  (but disconnected from all the others), has to be removed from  $T^{(n)}$  in order to obtain  $C^{(n)}$ , i.e., the term  $C^{(2)}(a_1, a_3) T^{(n-2)}(a_2, a_4, \dots)$ . The corresponding explicit expression is, however, equivalent to the one on the r.h.s. of Eq. (15). The same obviously holds when applying the above procedure to all remaining frequencies  $a_4, \dots$  and, hence, the total subtraction term originating from diagrams where the frequency  $a_1$  is connected to *only* one other frequency is given by  $n - 1$  (i.e., the number of frequencies to which  $a_1$  can be connected) times the expression on the r.h.s. in Eq. (15).

In the next step we will remove all diagrams from  $T^{(n)}$  where the frequency  $a_1$  is connected to *two* other frequencies but disconnected to the rest such as, e.g.,  $C^{(3)}(a_1, a_2, a_3) T^{(n-3)}(a_4, a_5, \dots)$ . Following the arguments from the previous paragraph, this yields  $(n - 1)(n - 2)/2$  (corresponding to the number of ways to select 2 frequencies from a set of  $n - 1$  frequencies) equivalent terms of the form  $\mathcal{C}_3 \mathcal{F}_{(n-3)} (\tilde{G}(a_1) - G(a_1)) \dots$  which have to be removed from  $T^{(n)}$ .

Extending the above arguments to one-particle disconnected diagrams where a number  $2 \leq l \leq n - 2$  frequencies are connected to the frequency  $a_1$  and all the others are disconnected from  $a$ , we obtain an subtraction term of the form  $\binom{n-1}{l-1} \mathcal{C}_l \mathcal{F}_{(n-l)} (\tilde{G}(a_1) - G(a_1)) \dots$ . We can, hence, obtain an explicit expression for  $C^{(n)}(a_1, a_2, a_3, \dots)$  by subtracting all the above mentioned contributions from the one-particle connected

function  $T^{(n)}(a_1, a_2, a_3, \dots)$  which yields

$$\begin{aligned} \mathcal{C}_n \left( \tilde{G}(a_1) - \tilde{G}(a_1) \right) \dots &= \mathcal{F}_n \left( \tilde{G}(a_1) - \tilde{G}(a_1) \right) \dots \\ &- \sum_{l=2}^{n-2} \binom{n-1}{l-1} \mathcal{C}_l \mathcal{F}_{n-l} \left( \tilde{G}(a_1) - \tilde{G}(a_1) \right) \dots \end{aligned} \quad (16)$$

Since the product of  $(\tilde{G} - G)$  appears for each summand in this equation it can be removed in each term which finally yields the following iterative expression for the determination of the prefactor  $\mathcal{C}_n$

$$\mathcal{C}_n = \mathcal{F}_n - \sum_{l=2}^{n-2} \binom{n-1}{l-1} \mathcal{C}_l \mathcal{F}_{n-l} \quad (17)$$

After the determination of  $\mathcal{C}_n$  from the above relations the connected  $n$ -particle Green's function is determined by Eq. (14).

In a final step we can now calculate the connected  $n$ -particle vertex function  $F^{(n)}$  from  $C^{(n)}$  by just amputating the external legs, i.e., via dividing by the corresponding one-particle Green's functions  $G^{(1)}(a)$ . By defining  $f(a)$

$$f(a) = (\tilde{G}(a) - G(a)) / (G^{(1)}(a))^2, \quad (18)$$

the explicit expression for the full  $n$ -particle vertex  $F^{(n)}$  is then given by

$$\begin{aligned} F^{(n)}(a_1, \dots, a_n, a_{n+1}, \dots, a_{2n}) \\ = \delta_{a_{n+1} \dots a_{2n}} \mathcal{C}_n f(a_1) \dots f(a_n). \end{aligned} \quad (19)$$

For  $n = 2$  this is equivalent to the corresponding expression found in Ref. 55.

### III. INVESTIGATING THE PROPERTIES OF $\mathcal{C}_n$

In this section we want to analyze the behavior of the prefactor  $\mathcal{C}_n$  for increasing  $n$  which can be considered as a first estimate for the “magnitude” of the vertex function of a certain order  $n$ . This is a relevant issue for various diagrammatic extensions of DMFT such as DF and 1PI which typically construct nonlocal corrections to the DMFT self-energy from the two-particle local vertex function assuming that all higher-order vertices are in some sense “small”. Hence, in order to obtain an understanding of the magnitude of  $\mathcal{C}_n$  we iterate Eq. (16) up to a given order  $n > 2$  starting from the initial conditions  $\mathcal{F}_2 = \mathcal{C}_2 = p_1 p_2$  (recall that  $p_1$  denotes the density of localized  $f$  electrons and  $p_2 = 1 - p_1$ ). In Figs. 2 and 3 we present our data for  $\mathcal{C}_n$  and  $\mathcal{F}_n$  up to  $n = 10$  for half<sup>79</sup> ( $p_1 = p_2 = 0.5$ ) and quarter ( $p_1 = 0.25, p_2 = 0.75$ ) filling, respectively. For these small values of  $n$ , the size of  $\mathcal{C}_n$  is still moderate. However, when extending the range  $n$  up to  $n = 20$  (for half-filling) we observe already

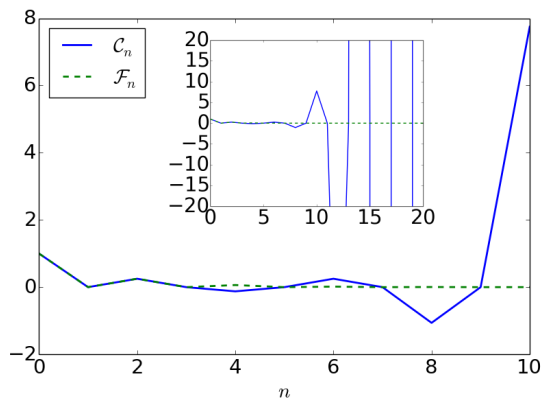


FIG. 2. (Color online) Coefficients  $\mathcal{C}_n$  ( $\mathcal{F}_n$ ) for the connected (one particle connected)  $n$ -particle Green's function at half-filling  $p_1 = p_2 = 0.5$  for  $n$  up to 10. The insert shows the behavior up to  $n = 20$ .

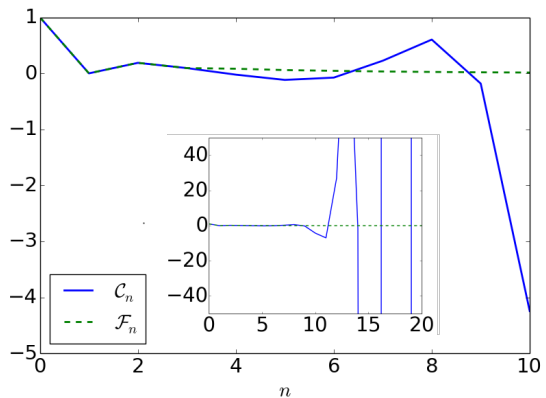


FIG. 3. (Color online) Same as Fig. 2 but for quarter filling  $p_2 = 0.25$ .

a much stronger increase of  $\mathcal{C}_n$  with  $n$  (see inset of Fig. 2). By increasing  $n$  further up to  $n = 200$  (see Fig. 4 for half- and Fig. 5 for quarter-filling) we find an extremely strong increase of  $\mathcal{C}_n$ : In fact, plotting  $\log|\mathcal{C}_n|$  (rather than  $\mathcal{C}_n$  itself) as it is done in these figures we observe an increase even stronger than linear on this logarithmic scale indicating that  $\mathcal{C}_n$  is growing faster than exponentially with  $n$ .

Let us provide an analytical understanding for this numerically observed growth rate of  $\mathcal{C}_n$  in the simple case of half-filling ( $p_1 = p_2 = 1/2$ ) where  $\mathcal{C}_n \equiv 0$  for all odd<sup>79</sup>  $n$  and, hence, the sum in Eq. (16) is restricted to even  $l$ . The binomial coefficient in this relation suggest a factorial growth of  $\mathcal{C}_n$ : In fact, considering the last term in this sum we obtain that  $\mathcal{C}_n \propto (n-1)(n-2)\mathcal{C}_{n-2}$ . Hence, we expect that,  $\mathcal{C}_n / [(n-1)(n-2)\mathcal{C}_{n-2}]$  of two neighboring (non-zero) coefficients in the recursion relation of

Eq. (16) should be constant for large values of  $n$ , i.e.,

$$r_n = \frac{\mathcal{C}_n}{\mathcal{C}_{n-2}(n-1)(n-2)}, \quad (20)$$

for  $n \rightarrow \infty$ . Fig. 6 shows the behavior of  $r_n$  as a function of  $n$ . We can clearly see that it approaches a constant value which can be numerically estimated as  $r_{n \rightarrow \infty} = r_a \approx -0.1$ . Note that the minus sign of this number reflects perfectly the alternating behavior of the sign of  $\mathcal{C}_n$  for neighboring (even)  $n$  observed in Fig. 2.

Eq. (20) can be now used as an iteration scheme which allows us to find an (approximate) explicit expression for  $\mathcal{C}_n$  at large values of  $n$ . It is given by

$$\mathcal{C}_n \cong K \sqrt{r_a}^{n-2} (n-1)!, \quad (21)$$

with some prefactor  $K$  (which should be fitted to the large- $n$  tail of  $\mathcal{C}_n$ ) and  $\cong$  indicates that this relation holds only for  $n \rightarrow \infty$ . We have then inserted the above form of  $\mathcal{C}_n$  into both sides of the recursion relation in Eq. (16) which yields (considering the simplifications occurring for  $n \rightarrow \infty$ )  $r_a = -1/\pi^2 \sim -0.1$ , coinciding exactly with the numerical prediction.

Eq. (21) demonstrates that  $\mathcal{C}_n$  grows -at half-filling-factorially with  $n$ . Let us, however, point out here that the above considerations and approximations cannot be directly transferred to situations out of half-filling due to the emergence of quasi-periodic structures in  $r$  as it can be observed in Fig. 6.

At a first glance the strong increase of the magnitude of the local DMFT vertex functions with the particle number might invalidate indeed the state-of-the-art diagrammatic extensions of DMFT such as DF and 1PI in their standard formulation, where they are restricted to the two-particle vertex level. Two further aspects, however, have to be considered which put the above argument in perspective: (i) The alternating behavior of the sign of  $\mathcal{C}_n$  (see Figs. 2 and 3) will certainly mitigate a strong growth of diagrammatic contributions upon increasing  $n$  in the before mentioned methods, and (ii) the larger number of Green's function in diagrams with higher order vertices might compensate the the increasing size of the vertex functions itself. The later issue will be discussed in more detail in the following section.

#### IV. ESTIMATE OF HIGHER ORDER VERTEX CONTRIBUTIONS

In following we will estimate how the factorial growth of the local  $n$ -particle vertex of the FKM discussed in the previous section will affect the magnitude of Feynmann diagrams for the partition function, which are constructed from such vertices in the framework of diagrammatic extensions of DMFT. To this end we will evaluate a generic partition function diagram assuming a general atomic-limit-like form of the Green's functions within the

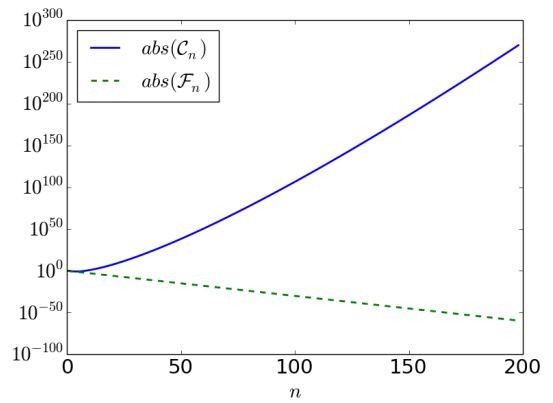


FIG. 4. (Color online) Coefficients  $abs(\mathcal{C}_n)$  ( $abs(\mathcal{F}_n)$ ) for the (one-particle) connected  $n$ -particle vertex at half-filling  $p_1 = p_2 = 0.5$  for even  $n$  up to 200. Note the logarithmic scale.

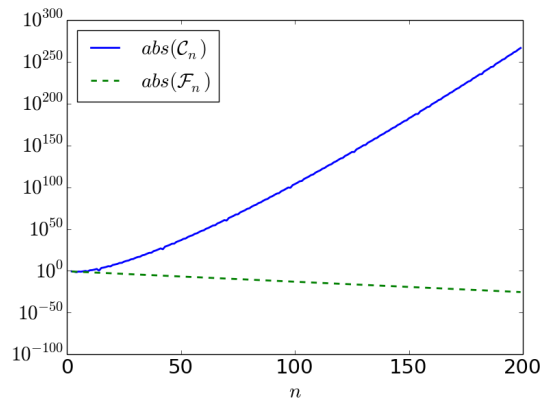


FIG. 5. (Color online) Same as Fig. 4, but for quarter-filling  $p_2 = 0.25$  and also including odd numbers for  $n$ .

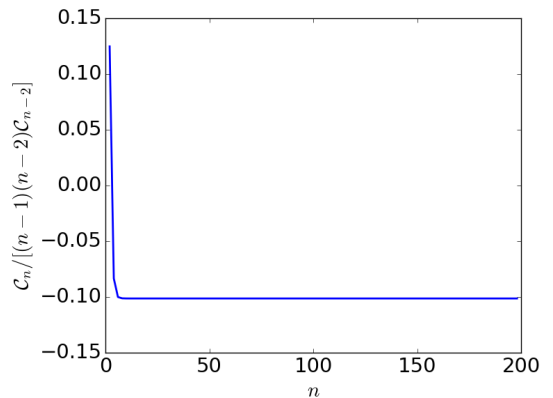


FIG. 6. (Color online) Ratio  $r_n = \mathcal{C}_n / [(n-1)(n-2)\mathcal{C}_{n-2}]$  at half-filling  $p_1 = p_2 = 0.5$ . Note that  $r_n$  converges towards a negative constant, implying an alternating sign of  $\mathcal{C}_n$  (for even  $n$ ).

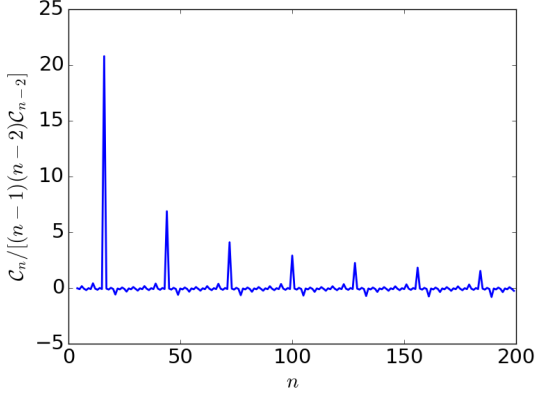


FIG. 7. (Color online) Same as Fig. 6, but for  $p_2 = 0.25$ . Away from half-filling, quasi-periodic structures arise in the ratio.

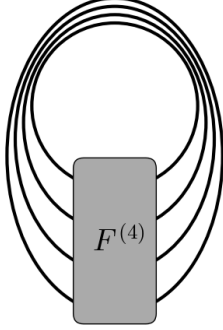


FIG. 8. (Color online) An exemplary diagram (“necklace” diagram) contributing to the partition function, which can be generated within a diagrammatic extension of DMFT such as DF or 1PI including the local 4-particle vertex function. Generalizations to corresponding diagrams with higher-order local vertices are straightforward.

dual fermion framework:

$$G_{\text{approx}}(\nu_l) \propto \frac{\bar{\varepsilon}}{\nu_l^2}, \quad (22)$$

where  $\nu_l = \pi T(2l - 1)$ ,  $l \in \mathbb{Z}$ .  $\bar{\varepsilon}$  is a characteristic energy scale of the system. The simplest diagrams for the partition function which can be constructed from this Green’s function and the  $n$ -particle vertex functions of DMFT are of first order in the  $n$ -particle vertex: They can be obtained by connecting all its entrances and exits pairwise by  $n$  one-particle Green’s functions  $G_{\text{approx}}$ . An example of such diagram adopting the  $n = 4$ -particle vertex is depicted in Fig. 8. In the following we will analyze the contribution of such diagrams to the partition function, which we will denote as  $\Omega^{(n)}$ , for large values

of  $n$ . Note that while the bare dual propagator does not have a local component, in a self-consistent dual fermion formulation, local contributions can appear due to self-energy corrections. The basic structure of these terms is given by<sup>26</sup>

$$\Omega^{(n)} \sim \sum_{\nu_1 \dots \nu_{2n}} G_{\text{approx}}(\nu_1) \dots G_{\text{approx}}(\nu_n) \times F^{(n)}(\nu_1, \dots, \nu_{2n}). \quad (23)$$

For this sum we have to keep in mind that the vertex  $F^{(n)}$  vanishes if two (incoming) frequency arguments  $a_1 \dots a_n$  take the same value. Consequently the largest contribution in the frequency sum in Eq. (23) is the one where each of the lowest  $n/2$  positive and negative Matsubara frequencies  $\pm \nu_1 \dots \pm \nu_{n/2}$  is attached to exactly one of the  $n$  Green’s functions. Assuming w.l.o.g. that  $n$  is even we can, hence, estimate the dominant contribution of the diagram in Fig. 8 (but for the case of a general even  $n$ ) as

$$\Omega^{(n)} \sim U^n \prod_{l=1}^{n/2} \left( \frac{\bar{\varepsilon}}{\nu_l^2} \frac{\bar{\varepsilon}}{\nu_l^2} \right) C_n = \frac{\beta^{2n} \bar{\varepsilon}^n U^n}{(2\pi)^{2n}} \prod_{l=1}^{n/2} \frac{1}{(2l-1)^4} C_n, \quad (24)$$

where we have replaced the full vertex  $F^{(n)}$  just by its prefactor  $C_n$  times  $U^n$ , which originates from the limiting value of  $f(a)$  for high frequencies. This is justified for a metallic like Green’s function since the contribution  $1/[G^{(1)}(\nu)]^2$ , present in the definition of  $F^{(n)}$  in Eq. (19), is non-zero and remains bounded for all frequencies.

Inserting now the asymptotic form of  $C_n$  as given in Eq. (21) into Eq. (24) yields (after some simple algebraic manipulations)

$$\Omega^{(n)} \sim K(U\beta^2 \bar{\varepsilon})^n \frac{\sqrt{r_a}^{n-2}}{\pi^{2n}} \frac{[(n/2-1)!]^4}{((n-1)!)^3} \quad (25)$$

Application of Stirling’s formula allows us to get rid of the factorial expressions.

$$\Omega^{(n)} \propto 4K(U\beta^2 \bar{\varepsilon})^n \frac{\sqrt{r_a}^{n-2}}{(2\pi)^{2n}} \frac{1}{n^{n-1} e^n} \quad (26)$$

The corresponding contribution to the partition function gets damped and the sum of such terms is (absolutely) convergent. Note that our approximation is only valid for the case  $T \gtrsim b$ , with  $b$  being the bandwidth of the system, as it relies on the asymptotic values of the vertex and Green’s function being reached. Certainly, the limit  $T \rightarrow 0$  cannot be taken. On one hand, this would violate our assumption that the first summand in terms of frequencies gives the dominant contribution to the sum, on the other hand the specific approximation employed for the Green’s functions is bound to introduce divergencies in such a case.

Finally, a remark is in order about other types of diagrams for the partition function than the ones discussed



above. To this end let us consider, e.g., a diagram where a second  $n$ -particle vertex is inserted. This leads to a factor  $\mathcal{C}_n^2$  rather than  $\mathcal{C}_n$ . However, also the number of the Green's functions in the diagram is doubled and, hence, the corresponding diagram behaves like the square of our evaluated value. In general, we can, hence, state that the diagram depicted in Fig. 8 and corresponding higher-order diagrams represent somehow the “worst case” regarding the convergence with large  $n$ . Hence, although the above calculation has been done for the rather specific case of the FKM using the vertex of the half-filled system it might be seen as a justification of the general restriction of the DF expansion to the lowest order vertex functions. This, however, does not guarantee that contributions for low  $n > 2$  are fully negligible, as we will demonstrate in the following section by including a  $n = 3$ -particle diagram for the calculation of DF self-energy corrections in the FK model.

## V. NUMERICAL RESULTS FOR 3<sup>rd</sup> ORDER TERMS WITHIN DUAL FERMION THEORY

In this section we present numerical results for the non-local corrections to the DMFT self-energy constructed from two- and three-particle local DMFT vertices within the DF approach. To this end we have considered the FKM at quarter  $f$ -filling ( $p_1 = 0.25$ ) for the parameters  $U = 1$ ,  $\mu = 0.2$  and a temperature of 0.05, resulting in a filling by  $c$ -electrons of  $\langle c^\dagger c \rangle \approx 0.53$  within DMFT. The diagrams including a three-particle vertex employed in the calculation are depicted in fig. 9. To this end we consider a diagram where four of the six outer legs of the local DMFT three-particle vertex  $F^{(3)}$  of the FKM are connected with a ladder built from two-particle vertices as depicted in Fig. 9. Since the  $F^{(3)}$  is purely local the corresponding self-energy correction will be also  $\mathbf{k}$ -independent, similar to the local correction term appearing within a 1PI calculation. The latter, in fact, represents just the contribution of Fig. 9 where instead of the full  $F^{(3)}$  only its one-particle reducible part is considered [see Ref. 20].

Unlike the 1PI-case however, the correction to the local self energy applies to the dual fermions, thereby indirectly influencing the self energy of the real fermions for different  $k$ -points in slightly different ways due to the mapping from dual- to real-fermion intermixing different contributions to the dual self-energy.

The explicit form of the dual self-energy corrections generated by the diagram in Fig. 9 is given by

$$\Sigma^3(k) = -\frac{1}{4} \sum_{k_1 k_2 q} F^{(3)}(k, k_1, k_2 + q, k, k_1 + q, k_2) \times \tilde{\mathcal{G}}(k_1) \tilde{\mathcal{G}}(k_1 + q) F^{(2)}(k_1, k_2 + q, k_1 + q, k_2) \tilde{\mathcal{G}}(k_2) \tilde{\mathcal{G}}(k_2 + q), \quad (27)$$

where  $k$ ,  $k_1$ ,  $k_2$  and  $q$  represent either 4-vectors including Matsubara-frequencies as well as wave vectors (for the Green's functions) or only Matsubara frequencies (for

the three-particle vertex  $F^{(3)}$ ).  $\tilde{\mathcal{G}}$  corresponds to the bare dual Green's function as given, e.g., in Ref. 55.  $F_q$  is the  $ph$ -ladder of the dual fermion theory which also has been already derived in Ref. 55. For  $F^{(3)}$  we will adopt the expression derived previously in Eq. 19 for  $n = 3$ . The factor in front of the sum accounts for the overcounting due to the exchangeability of the lines entering and leaving the two-particle vertex.

Considering the definition of the generalized susceptibility

$$\tilde{\chi}_{0,q}^{\nu_1, \nu_2} = \sum_{k_1} \tilde{\mathcal{G}}(\nu_1, k_1) \tilde{\mathcal{G}}(\nu_2, k_1 + q), \quad (28)$$

the explicit evaluation of Eq. (27) yields

$$\Sigma^3(\nu) = -\frac{1}{2} \sum_{\nu_1, \nu_2, \omega, k_1, k_2, q} F^{(3)}(\nu, \nu_1, \nu_2 + \omega, \nu, \nu_1 + \omega, \nu_2) \times \tilde{\chi}_{0,q}^{\nu_1, \nu_1 + \omega} \left( F_q^{\nu_1, \nu_2, \omega} - \frac{1}{2} F^{(2)}_{\nu_1, \nu_2, \omega} \right) \tilde{\chi}_{0,q}^{\nu_2, \nu_2 + \omega} \quad (29)$$

where  $F^{(2)}$  was written down in  $ph$ -notation. Note how the factor in front changed, because the  $ph$  and  $\overline{ph}$ -ladder contribute equally to the self energy, albeit via topologically distinct diagrams. The correction due to the local vertex is then overcounted and needs to be taken into account separately. Utilizing the frequency structure, especially the factorization of  $F^{(3)}$ , we can now express the self-energy correction in terms of two auxiliary matrices

$$X(\nu_1, \nu_2) = a(\nu_1) a(\nu_2) \sum_q \tilde{\chi}_{0,q}^{\nu_1, \nu_1} \left( F_q^{\nu_1, \nu_2, 0} - \frac{1}{2} F_{loc}^{\nu_1, \nu_2, 0} \right) \times \tilde{\chi}_{0,q}^{\nu_2, \nu_2} \quad (30)$$

$$Y(\nu_1, \nu_2) = -a(\nu_1) a(\nu_2) \sum_q \tilde{\chi}_{0,q}^{\nu_1, \nu_2} \left( F_q^{\nu_1, \nu_1, \nu_2 - \nu_1} - \frac{1}{2} F_{loc}^{\nu_1, \nu_2, \nu_2 - \nu_1} \right) \tilde{\chi}_{0,q}^{\nu_1, \nu_2} \quad (31)$$

For calculating the self-energy corrections, all admissible values of  $\nu_1$  and  $\nu_2$  have to be summed over

$$\Sigma^3(\nu) = \mathcal{C}_3 a(\nu) \sum_{\nu_1, \nu_2 | \nu \neq \nu_1 \neq \nu_2 \neq \nu} [X(\nu_1, \nu_2) + Y(\nu_1, \nu_2)]. \quad (32)$$

In Fig. 10, different corrections terms within 1PI and DF are given. The DMFT self-energy shows usual behaviour, with a Hartree-term proportional to  $p_1 U$  as asymptotic value. The expressions for the correction to the DMFT self-energy within 1PI and the dual self-energy within DF on the two-particle vertex level are very similar, in fact only differing by the propagator used to close a loop in the respective diagram. Those two propagators differ by the local DMFT Green's function. Note, however, that the dual self-energy needs to be mapped back to extract a real self-energy, so some care needs to be taken when

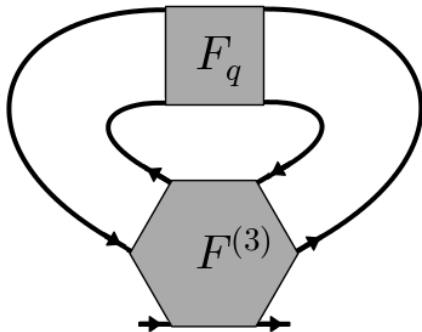


FIG. 9. Diagrammatic representation of correction to local  $\Sigma$  due to a 3-particle vertex.

comparing the two quantities. The additional contribution within 1PI leads to a local correction term for the self-energy on the level of two-particle vertices. Diagrammatically, 1PI is known to introduce corrections to the self-energy stemming from one-particle reducible contributions to the three-particle vertex already within the terms constructed from two-particle vertices. This leads us to compare the terms due to three-particle vertices within DF-theory to the additional terms appearing in 1PI already on the two particle level. Unlike 1PI, the third order DF renormalizes the Hartree term.

The two-particle order corrections to the dual self-energy are  $k$ -dependent, they are given for 4 points of high symmetry-  $(0,0)$ ,  $(0,\pi)$ ,  $(\pi/2,\pi/2)$  and  $(\pi,\pi)$ . The corrections are of the same order of magnitude for all four  $k$ -points. Notably, the corrections due to the three-particle vertex are of the same order of magnitude. Thus, a truncation of the DF approach on the two-particle level does not seem justified for this set of parameters.

## VI. CONCLUSION

We have derived analytical expressions for the  $n$ -particle DMFT Green's function of the FKM and from this, by removing all disconnected Feynman diagrams,

for the full  $n$ -particle vertex. This main result of our paper can be found in Eq. (19). While it was known before that the  $n=3$ -particle vertex vanishes at half-filling, we show that this is indeed the case for all odd  $n$ , whereas it is finite for even  $n$ . Our analysis of the prefactor for the vertex reveals that it grows post exponentially, which is partially compensated by a fluctuating sign of this prefactor.

The calculated local vertex serves as a starting point for diagrammatic extensions of DMFT such as the DF, DFA and 1PI approach. The latter two require the fully irreducible and the one-particle irreducible vertex, respectively, whereas the DF approach is based on the full vertex which we calculated. Hitherto, these approaches have been restricted to the  $n=2$ -particle vertex which is the main approximation of these diagrammatic extensions. Our calculation of the local vertex for arbitrary  $n$  now allows us to go beyond this approximation. Or at least we can now estimate the error of the restricting to the 2-particle vertex in DF by estimating the magnitude of higher order vertex contributions.

If one connects to this end the  $n$ -particle vertices by Green function lines in the DF approach, our order of magnitude estimate by hands of selected diagrams indicates that the series of DF contributions should be absolutely convergent despite the diverging prefactor. We also calculate the contribution of some exemplary ring diagrams which are based on the 3-particle vertex plus ladder (see Fig. 9). Our numerical results show that this selected DF contribution stemming from the 3-particle vertex is of the same magnitude as the standard DF ladder contributions based on the 2-particle vertex.

## VII. ACKNOWLEDGMENTS

The plots were made using the matplotlib<sup>77</sup> plotting library for python. Financial support is acknowledged from the Austrian Science Fund (FWF) through I-610-N16 as part of the DFG research unit FOR 1346 (GR,KH) and the European Research Council under the European Union's Seventh Framework Program (FP/2007-2013)/ERC through grant agreement n. 306447 (TR, KH).

<sup>1</sup> W. Metzner and D. Vollhardt, Phys. Rev. Lett. **62** 324 (1989).

<sup>2</sup> E. Müller-Hartmann, Z. Phys. B **74** 507 (1989).

<sup>3</sup> A. Georges and G. Kotliar, Phys. Rev. B **45** 6479 (1992).

<sup>4</sup> M. Jarrell, Phys. Rev. Lett. **69** 168 (1992).

<sup>5</sup> A. Georges, G. Kotliar, W. Krauth and M. Rozenberg, Rev. Mod. Phys. **68** 13 (1996).

<sup>6</sup> G. Kotliar, S. Y. Savrasov, K. Haule, V. S. Oudovenko, O. Parcollet, and C. A. Marianetti, Rev. Mod. Phys. **78**, 865 (2006).

<sup>7</sup> K. Held, Advances in Physics **56**, 829 (2007).

<sup>8</sup> M. H. Hettler, A. N. Tahvildar-Zadeh and M. Jarrell, Phys. Rev. B **58** 7475 (R) (1998).

<sup>9</sup> G. Kotliar, S. Y. Savrasov, G. Pálsson and G. Biroli, Phys. Rev. Lett. **87** 186401 (2001).

<sup>10</sup> A. I. Lichtenstein and M. I. Katsnelson, Phys. Rev. B **62** 9283 (R) (2000).

<sup>11</sup> T. Maier, M. Jarrell, T. Pruschke and M. H. Hettler, Rev. Mod. Phys. **77** 1027 (2005).

<sup>12</sup> A. Toschi, A. A. Katanin, and K. Held, Phys. Rev. B **75**, 045118 (2007); Prog. Theor. Phys. Suppl. **176**, 117 (2008).

<sup>13</sup> H. Kusunose, J. Phys. Soc. Jpn **75**, 054713 (2006).

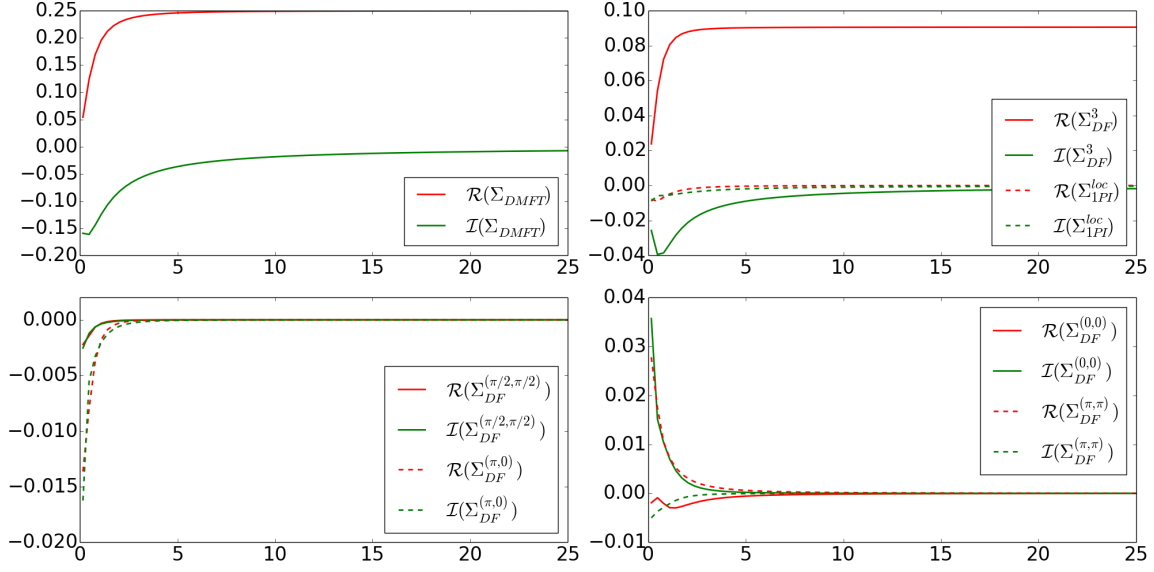


FIG. 10. (Color online) Upper left: Self energy  $\Sigma$  in DMFT for the square lattice FKM at quarter filling  $p_2 = 0.25$ ,  $U = 1$ , and  $T = 0.05$ . Upper right: Contribution of the local diagrams based on the 3-particle vertex in Fig. 9 (denoted as  $\Sigma^3$ ) and the comparison to the local 1PI correction ( $\Sigma^{1PI}$ ) in a standard calculation based on the 2-particle vertex. Lower panels: Standard DF correction to the self energy ( $\Sigma^{DF}$ ) for four different  $k$ -points. Note that the correction term from the 3-particle vertex is of similar magnitude as the contributions from the conventional 2-particle vertex in DF.

- <sup>14</sup> A. A. Katanin, A. Toschi, and K. Held, Phys. Rev. B **80**, 075104 (2009).  
<sup>15</sup> A. N. Rubtsov, M. I. Katsnelson, and A. I. Lichtenstein, Phys. Rev. B **77**, 033101 (2008).  
<sup>16</sup> A. N. Rubtsov, M. I. Katsnelson, and A. I. Lichtenstein, Annals of Physics **327**, 1320 (2012).  
<sup>17</sup> K. Held, "Dynamical vertex approximation", in E. Pavarini, E. Koch, D. Vollhardt, A. Lichtenstein (Eds.): "Autumn School on Correlated Electrons. DMFT at 25: Infinite Dimensions", Reihe Modeling and Simulation, Vol. 4 (Forschungszentrum Jülich, 2014) [arXiv:1411.5191].  
<sup>18</sup> A. Toschi, G. Rohringer, A. A. Katanin, and K. Held, Annalen der Physik, **523**, 698 (2011).  
<sup>19</sup> G. Li, Phys. Rev. B **91**, 165134 (2015).  
<sup>20</sup> G. Rohringer, A. Toschi, H. Hafermann, K. Held, V.I. Anisimov, A. A. Katanin, Phys. Rev. B **88**, 115112 (2013).  
<sup>21</sup> C. Taranto, S. Andergassen, J. Bauer, K. Held, A. Katanin, W. Metzner, G. Rohringer, A. Toschi, Phys. Rev. Lett. **112**, 196402 (2014).  
<sup>22</sup> T. Ayrar and O. Parcollet Phys. Rev. B **92**, 115109 (2015).  
<sup>23</sup> T. Ayrar and O. Parcollet, Phys. Rev. B **94**, 075159 (2016).  
<sup>24</sup> M. Kitatani, N. Tsuji, and H. Aoki, Phys. Rev. B **92**, 085104 (2015).  
<sup>25</sup> Here we have used the symmetric Fourier transform between the Matsubara time and the Matsubara frequency space, i.e.,  $(1/\sqrt{\beta}) \int_0^\beta d\tau \dots$  for the Fourier transform and  $(1/\sqrt{\beta}) \sum \nu \dots$  for the inverse Fourier transform. This convention is convenient for the decomposition of the  $n$ -particle Green's function into its connected and unconnected parts in the FKM as performed in the following, since it avoids any prefactors  $\beta^n$  in the definition of  $G^{(n)}$  in frequency space.

- <sup>26</sup> Note that the sum should in principle run over  $\nu_1 \dots \nu_{2n}$  since the  $n$ -particle Green's function  $G^{(n)}$  (and, hence, also  $G^{(1)}$ ) depends on frequencies  $\nu_1 \dots \nu_n$  (i.e., on  $\nu_1$  and  $\nu_2$  for  $G^{(1)}$ ). Considering the convention we used for the Fourier transform in [25] this yields a prefactor  $1/\sqrt{\beta}^{2n} = 1/\beta^n$ . Moreover, in Eq. (23) we have already performed the sums over  $\nu_{n+1} \dots \nu_{2n}$  which just eliminates the corresponding  $\delta$ -functions in the definition of the Green's function.  
<sup>27</sup> G. Rohringer, A. Toschi, A. A. Katanin, and K. Held, Phys. Rev. Lett. **107**, 256402 (2011).  
<sup>28</sup> D. Hirschmeier, H. Hafermann, E. Gull, A. I. Lichtenstein, and A. E. Antipov, Phys. Rev. B. **92**, 144409 (2015).  
<sup>29</sup> T. Schäfer, A. A. Katanin, K. Held, and A. Toschi, arXiv:1605.06355.  
<sup>30</sup> A. E. Antipov, E. Gull, and S. Kirchner, Phys. Rev. Lett. **112**, 226401 (2014).  
<sup>31</sup> T. Schäfer, F. Geles, D. Rost, G. Rohringer, E. Arrigoni, K. Held, N. Blümer, M. Aichhorn, and A. Toschi, Phys. Rev. B **91**, 125109 (2015).  
<sup>32</sup> Besides, there is also the question of which diagrams to generate with the local two-particle vertex as a starting point. Here, in principle, the parquet equations<sup>33,34</sup> or the diagrammatic Monte Carlo approach<sup>35</sup> are the most extensive since they generate all Feynman diagrams for a given fully irreducible vertex. But in practice more often simpler ladder diagrams are summed up, with a few noteworthy exceptions solving the parquet equations.<sup>36-40</sup>  
<sup>33</sup> C. De Dominicis, J. Math. Phys. **3**, 983 (1962); C. De Dominicis and P. C. Martin, **5**, 14 (1964).  
<sup>34</sup> J. Bickers, Chap 6 in *Theoretical Methods for Strongly Correlated Electrons*, eds. D. Senechal, A.M. Tremblay, and C. Bourbonnais (Springer, New York, 2004).

- <sup>35</sup> S. Isakov, A. E. Antipov, and E. Gull, Phys. Rev. B **94**, 035102 (2016).
- <sup>36</sup> S. X. Yang, H. Fotso, J. Liu, T. A. Maier, K. Tomko, E. F. D'Azevedo, R. T. Scalettar, T. Pruschke, and M. Jarrell, Phys. Rev. E **80**, 046706 (2009).
- <sup>37</sup> Ka-Ming Tam, H. Fotso, S.-X. Yang, Tae-Woo Lee, J. Moreno, J. Ramanujam, and M. Jarrell, Phys. Rev. E **87**, 013311 (2013).
- <sup>38</sup> A. Valli, T. Schäfer, P. Thunström, G. Rohringer, S. Andergassen, G. Sangiovanni, K. Held, and A. Toschi, Phys. Rev. B **91**, 115115 (2015).
- <sup>39</sup> G. Li, N. Wentzell, P. Pudleiner, P. Thunström, and K. Held, Phys. Rev. B **93**, 165103 (2016).
- <sup>40</sup> V. Janiš, A. Kauch, and V. Pokorný, arXiv:1604.01678.
- <sup>41</sup> G. Rohringer, A. Valli, and A. Toschi, Phys. Rev. B **86**, 125114 (2012).
- <sup>42</sup> A. Rubtsov and A. Lichtenstein, Journal of Experimental and Theoretical Physics Letters **80**, 61 (2004).
- <sup>43</sup> P. Werner, A. Comanac, L. de' Medici, M. Troyer, and A. J. Millis, Phys. Rev. Lett. **97**, 076405 (2006).
- <sup>44</sup> E. Gull, A. J. Millis, A. I. Lichtenstein, A. N. Rubtsov, M. Troyer, and P. Werner, Rev. Mod. Phys. **83**, 349 (2011).
- <sup>45</sup> P. Gunacker, M. Wallerberger, E. Gull, A. Hausoel, G. Sangiovanni, and K. Held, Phys. Rev. B **92**, 155102 (2015).
- <sup>46</sup> P. Gunacker, M. Wallerberger, T. Ribic, A. Hausoel, G. Sangiovanni, and K. Held, arXiv:1607.01211.
- <sup>47</sup> L. M. Falicov and J. C. Kimball, Phys. Rev. Lett. **22**, 997 (1969).
- <sup>48</sup> U. Brandt and C. Mielsch, Z. Phys. B: Condens. Matter **75**, 365 (1989).
- <sup>49</sup> J. K. Freericks and V. Zlatić, Rev. Mod. Phys. **75**, 1333 (2003).
- <sup>50</sup> P.G.J. van Dongen and D. Vollhardt, Phys. Rev. Lett. **65**, 1663 (1990).
- <sup>51</sup> J. K. Freericks and P. Miller, Phys. Rev. B **62**, 10022 (2000).
- <sup>52</sup> V. Janiš and V. Pokorný, Phys. Rev. B **81**, 165103 (2010).
- <sup>53</sup> V. Pokorný and V. Janiš, J. Phys.: Condens. Matter **25**, 175502 (2013).
- <sup>54</sup> A. E. Antipov, Y. Javanmard, P. Ribeiro and S. Kirchner Phys. Rev. Lett. **117** 146601 (2016).
- <sup>55</sup> T. Ribic, G. Rohringer and K. Held, Phys. Rev. B **93** 195105 (2016).
- <sup>56</sup> A. M. Shvaika, Physica C **341**, 177 (2000).
- <sup>57</sup> M. Plischke, Phys. Rev. Lett. **28**, 361 (1972).
- <sup>58</sup> J. Hubbard, Proc. R. Soc. London, Ser. A **276**, 238 (1963).
- <sup>59</sup> U. Brandt and R. Schmidt, Z. Phys. B: Condens. Matter **63**, 45 (1986).
- <sup>60</sup> T. Kennedy and E. Lieb, Physica A **138**, 320 (1986).
- <sup>61</sup> J. K. Freericks, C. Gruber, and N. Macris, Phys. Rev. B **53**, 16189 (1996).
- <sup>62</sup> J. K. Freericks, E. H. Lieb, and D. Ueltschi, Phys. Rev. Lett. **88**, 106401 (2002).
- <sup>63</sup> V. Janiš, Z. Physik B **83**, 227 (1991).
- <sup>64</sup> A. Schiller and K. Ingersent, Phys. Rev. Lett. **75** 113 (1995).
- <sup>65</sup> M. Potthoff, M. Aichhorn and C. Dahnken, Phys. Rev. Lett. **91** 206402 (2003).
- <sup>66</sup> A. Schiller, Phys. Rev. B **60**, 15660. (1999).
- <sup>67</sup> M. H. Hettler, M. Mukherjee, M. Jarrell, and H. R. Krishnamurthy, Phys. Rev. B **61**, 12739 (2000).
- <sup>68</sup> A. N. Rubtsov, M. I. Katsnelson, A. I. Lichtenstein, and A. Georges, Phys. Rev. B **79**, 045133 (2009).
- <sup>69</sup> V. Janiš, Phys. Rev. B **64**, 115115 (2001).
- <sup>70</sup> A. A. Katanin, J. Phys. A: Math. Theor. **46**, 045002 (2013).
- <sup>71</sup> P. G. J. van Dongen and C. Leinung, Ann. Phys. (Leipzig) **509**, 45 (1997).
- <sup>72</sup> V. Janiš and D. Vollhardt, Phys. Rev. B **63**, 125112 (2001).
- <sup>73</sup> T. Schäfer, G. Rohringer, O. Gunnarsson, S. Ciuchi, G. Sangiovanni, and A. Toschi, Phys. Rev. Lett. **110**, 246405 (2013).
- <sup>74</sup> V. Janiš and V. Pokorný, Phys. Rev. B **90**, 045143 (2014).
- <sup>75</sup> M.M. Maška, and K Czajka, Phys. Rev. B. **74**, 035109 (2006).
- <sup>76</sup> Y.M. Vilk and A.-M.S. Tremblay, J. Phys. I France **7**, 1309 (1997).
- <sup>77</sup> J. D. Hunter, Computing In Science & Engineering **9**(3):90–95 (2007).
- <sup>78</sup> Note that there are of course diagrams which are 1PD in more than one frequency. In fact, an unconnected diagram consisting of a product of  $n$  one-particle Green's functions belongs also to this class and is 1PD in all its frequency arguments.
- <sup>79</sup> Note that for half-filling and  $C_n$  vanishes for all odd numbers  $n$ . This can be readily proved by induction considering the vanishing of  $\mathcal{F}_n$  for all odd  $n$  [see Eq. (7)].